Acoustic inerter: Ultra-low frequency sound attenuation in a duct

Yongzhen Mi, [1]Zhenbo Lu, [2,3] and Xiang Yu [1, a)]

[1] *Institute of High Performance Computing, A*STAR, Singapore, 138632*

2 *School of Aeronautics and Astronoautics, Sun Yat-Sen University, P.R China, 510275*

3 *Temasek Laboratories, National University of Singapore, Singapore, 117411*

Abstract

This letter reports a new class of acoustic metamaterial exhibiting a unique sound pressure amplification mechanism for ultra-low frequency sound attenuation. The system is constructed by integrating a flexible panel into the side-branch duct of a Herschel-Quincke (HQ) tube. A new peak emerges in the Sound Transmission Loss (STL), at a frequency far lower than the frequencies of the HQ tube-induced STL peaks. Neither can it, after careful comparisons, be attributed to any local resonances, including structural resonances of the flexible panel or air resonances inside the side-branch cavities. To explain the underlying physics, several numerical simulations are performed. The results reveal that analog to a mechanical inerter, a "push-pull" force is created by the sound pressure difference between the sub-cavities, in which a pressure amplification mechanism is generated at the interface of the embedded panel. This force is large enough to activate an out-of-plane motion of the flexible panel, trapping the incident sound power in a circulation around the duct-branch loop. The unique phenomenon is successfully reproduced in experiment, where the flexible panel is made of carbon fiber. The proposed acoustic metamaterial can be used as silencing components for ultra-low frequency noise control in duct.

[a)] Author to whom correspondence should be addressed: yuxiang@ihpc.a-star.edu.sg

I. Introduction

Attenuating sound in the very low-frequency region is challenging. Acoustic ducts, widely used to achieve that goal, must be long enough to match the acoustic wavelength. Attenuating a very low-frequency sound renders an unrealistically long, and thus physically unachievable duct. Acoustic metamaterial has been proposed as a new way to solve the problem, which typically consists of periodic Helmholtz resonators as side-branches along a duct.[1-3] The collective resonance of those resonators, whose frequency could be tuned as desired, causes substantial attenuation of the incoming sound and creates a peak in the Sound Transmission Loss (STL) of the duct.[4-6] However, although this peak is high, it only spans a quite narrow frequency range, limiting the practicality of the acoustic metamaterial.[7-9] Therefore, many researchers are investigating alternatives,[10-12] among which the membrane-type acoustic metamaterial has attracted massive attentions.[13-15] This new type replaces the Helmholtz resonator with a pre-stretched membrane decorated by a centered mass. The pliable membrane makes the stop band of the acoustic metamaterial starts at a low frequency, and the centered mass helps maintain the stop band over a wide band.[16,17]

However, the membrane-type acoustic metamaterial is not an ideal solution. The membrane is vulnerable to loading, heat and chemical erosion.[18] Its in-duct installation also obstructs fluid flow or air ventilation. This motivates us to seek a new mechanism for acoustic metamaterial design, referred to as "acoustic inerter" that is similar to the mechanical inerter. The idea of "inerter" was first introduced in the area of vibration isolation, as a new way to design vehicle suspensions.[19] It generates an inertial force proportional to the relative acceleration between the excitation and the receiver, through an inertia-like coefficient that could be larger than the system's actual mass.[20,21] The inerter couples the mass of its two ports through its inertance, just as a spring

element couples the stiffness of its two ports through its compliance. Later, the inerter was used in phononic crystals,[22-25] and was further employed for longitudinal vibration control in rods.[26] The inerter was then transformed to an equivalent bar-and-hinge mechanism and periodically embedded on a host beam, creating a wide stop band of flexural waves in the low frequency region.[27-29] Likewise, the inerter could also be realized, acoustically, as a side-branch duct segregated by a flexible panel and connected by two nodes to a main duct, manifesting the Herschel-Quincke (HQ) tube-shaped acoustic inerter as we initiated in this paper.[30] A classical HQ tube uses the longer-travelled, and thus phase-lagged, side-branch sound waves to cancel those in the main-duct, destructing all sound waves before they arrive at the outlet. We will demonstrate the low-frequency performance of the acoustic inerter through numerical simulations and experimental investigations. An explanation of its working mechanism will also be provided.

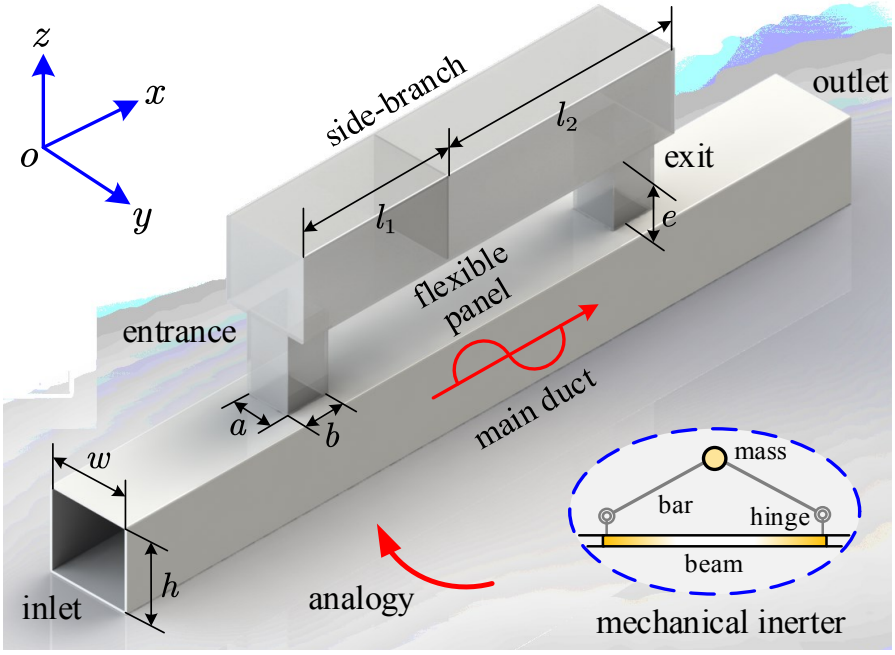

FIG. 1. Schematic of the acoustic inerter with pressure amplification mechanism. The inset shows analogy to a mechanical inerter.

II. Simulation and experiment

A schematic of the proposed acoustic inerter is shown in Fig. 1. It is built by segregating the side-branch of a HQ tube with a flexible panel, mimicking the mechanical inerter shown in the inset of Fig. 1. The main duct and the side-branch have same cross-sectional dimensions of $h = w = 0.1$ m. The entrance and exit of the side-branch also have same cross-sectional dimensions of $a = b = 0.05$ m. Their height is $e = 0.1$ m. The lengths of the side-branch before and after the flexible panel are $l_1 = 0.2$ m and $l_2 = 0.3$ m. The flexible panel is made of carbon-fiber, with density $\rho_s = 2000$ kg/m^3, Young's modulus $E = 70$ GPa, Poisson's ratio $\nu = 0.3$, and thickness $t = 0.3$ mm. Its four edges are seamlessly constrained by the side-branch walls with simply-supported boundary conditions. The flow medium inside the acoustic inerter is air, characterized by its density $\rho_f = 1.225$ kg/m^3 and speed of sound $c_0 = 340$ m/s. The coordinate system has its origin at the center of the main duct inlet.

A three-dimensional finite element model of the acoustic inerter is developed using the commercial package COMSOL Multiphysics 5.4. The acoustic cavities are meshed by linear tetrahedral elements with element size of 5 cm, delivering an accurate result up to 1000 Hz. The flexible panel is uniformly discretized to triangular shell elements, whose front and back surfaces are subjected to full structural-acoustic coupling boundary conditions. Harmonic plane wave is excited at the inlet, propagates along either the main duct or the side-branch without viscous dissipation, and reaches the outlet where it is totally absorbed by a perfectly matched layer. A frequency response analysis is carried out from 10 to 500 Hz with a resolution of 5 Hz. As a key performance indicator of the acoustic inerter, the STL is calculated from the logarithmic ratio between the incident and transmitted sound power.

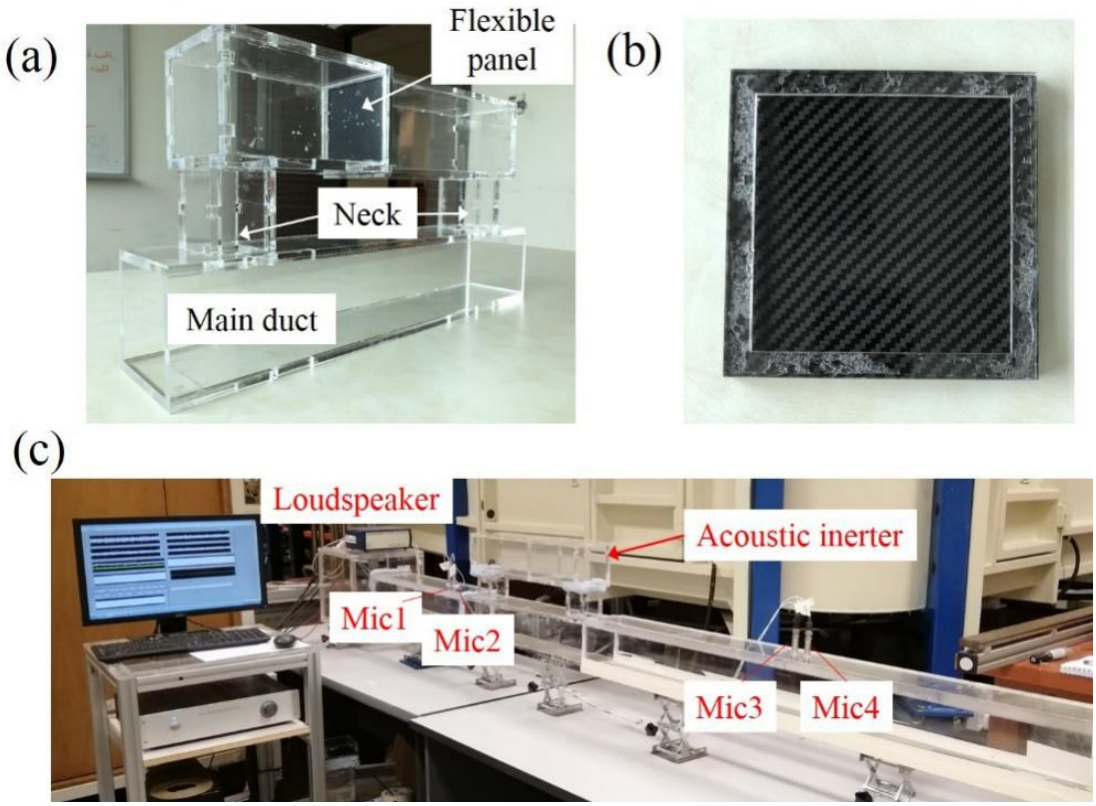

FIG. 2. (a) An acoustic inerter prototype. (b) The carbon-fiber panel that segregates the sub-branch. (c) Experimental set-up for STL measurement of the acoustic inerter.

The acoustic inerter prototype made by using acrylic material and laser cutting is shown in Fig. 2(a). A close view of the carbon-fiber panel is given in Fig. 2(b). The STL of this prototype was measured using the experiment set-up shown in Fig. 2(c). It consists of an in-house built impedance tube with two pairs of microphones (model 130E20, PCB Piezotronics) positioned before and after the test piece respectively. Signals from these microphones were recorded during a two-load measurement (open-end and semi-anechoic terminations), and further processed to give the STL. Removing that panel simplifies the acoustic inerter to a HQ tube, whose STL was measured in a same way.

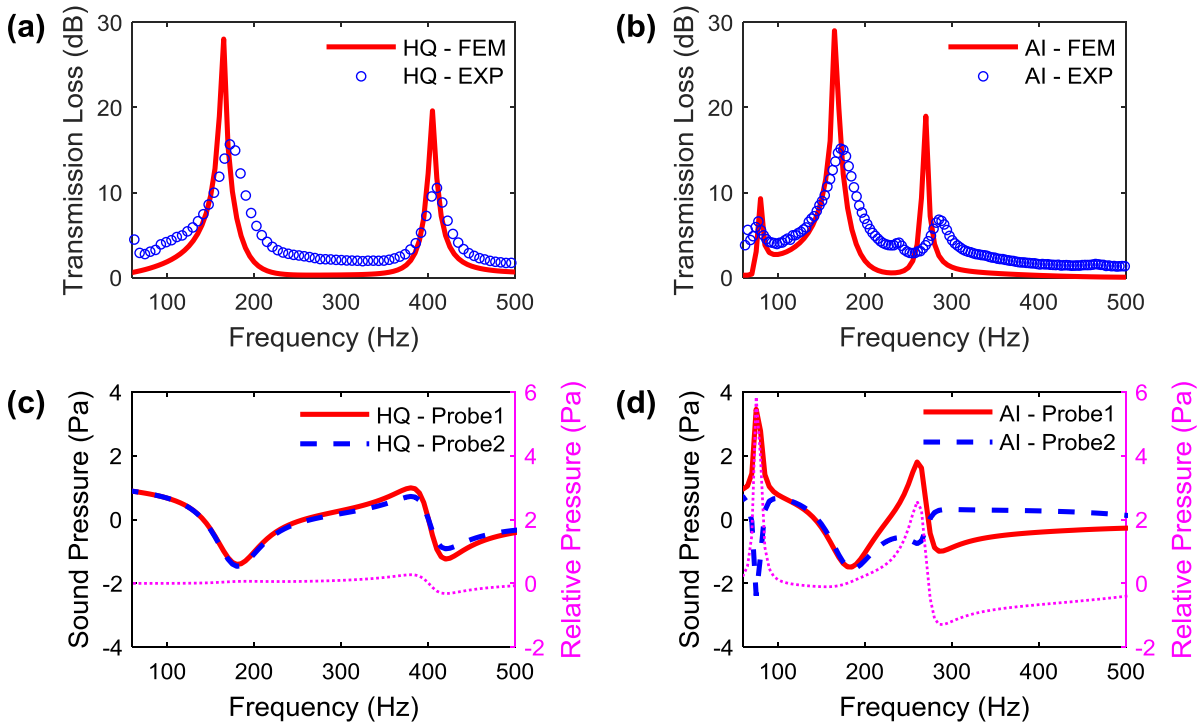

FIG. 3 (a) Simulated (solid curve) and measured (circle) STLs of the HQ tube. (b) Simulated (solid curve) and measured (circle) STLs of the acoustic inerter. (c) Simulated sound pressures (real part) at two points on the axis of the HQ tube side-branch and their difference (dotted curve). Probe 1 (solid line) and Probe 2 (dashed line) have the same distance with the location of the flexible panel. (d) Simulated sound pressures (real part) at the centers of cross-sectional surfaces (Probe 1 before the panel, solid line; Probe 2 after the panel, dashed line) in the acoustic inerter and their difference (dotted curve). In all figures, HQ denotes the HQ tube and AI the acoustic inerter.

III. Results and discussions

The simulated STL of the HQ tube is shown in Fig. 3(a) against its experimental counterpart. Two curves are in good agreement, except small mismatches probably caused by imperfections of the in-house built impedance tube. It can be seen that destructive interferences create two peaks at 170 Hz and 400 Hz, where the magnitude and phase of the volumetric flow from the side-branch cancels that of the wave propagating along the main duct.[30] Inserting the flexible panel transforms

the HQ tube to the acoustic inerter, whose simulated and measured STLs are shown in Fig. 3(b). Comparing to the HQ tube STL, one can notice that the two distinct peaks remain, but a new peak emerges interestingly at 80 Hz. Given its low-frequency nature, a reasonable hypothesis would be the new peak is attributed to some local resonances, either structural resonances of the flexible panel or air resonances inside side-branch sub-cavities. The analytical formula for the (M,N)-th order natural frequency of a simply-supported panel is expressed as $f_{(M,N)} = (\pi/2)\sqrt{D/\rho_s t}\,[(M/w)^2 + (N/h)^2]$ $(M,N = 1, 2, \cdots)$, where $D = Et^3/[12(1-\nu^2)]$ is the flexural rigidity. Coupling with fluid medium with a very low mass density—in this case, air—usually alters those natural frequencies slightly. Using this formula yields the lowest natural frequency of the panel, the $(1, 1)$-order, at 180 Hz, which is much higher than the frequency of the new peak. On the other hand, the two sub-cavities of the side-branch, if the panel is assumed as acoustically rigid, form two Helmholtz resonators. Their resonance frequencies can be approximately determined by $f_i = ic_0/4l$, $i = 1, 3, \cdots$, in which l is the length of the resonator. This formula gives the lower one at 210 Hz, which still deviates largely from that frequency. Thus, the new peak emerged at 80 Hz must be attributed to some traditionally unknown mechanism.

For further study, we draw in Fig. 3(d) the sound pressures at the centers of two surfaces before and after the flexible panel (probe 1 and probe 2, respectively, both 0.02 m away from the panel). Sound pressures inside the HQ tube at the same locations are given in Fig. 3(c). In both figures, the relative pressures of the two points are also plotted. While the sound pressure barely changes from probe 1 to probe 2 in the HQ tube, the relative pressure of the two probes in the acoustic inerter undergoes a much stronger fluctuation over the whole frequency range. This strong fluctuation is manifested by two extremums at 80 and 270 Hz. By contrast, the relative pressure is almost null at 170 Hz, which reveals that the attenuation mechanism of the second rising peak at

170 Hz is similar to that of the HQ tube. The other two peaks at 80 and 270 Hz must be relevant to the involvement of the flexible panel.

The peak at 80 Hz has more physical significances, since effective STL at such an ultra-low frequency is usually hard to achieve. To explain this peak, a careful inspection of Fig. 3(d) found that the extremum at 80 Hz is much higher than that at 270 Hz. At 80 Hz, the sound pressure experiences a much larger phase change across the panel—sound pressures of probe 1 and probe 2 are almost in 180° out of phase. This phenomenon has brought us back to the definition of the inerter, where in mechanical system, an *inerter* is a two-node, one-port system where equal and opposite force applied at the nodes is proportional to the relative acceleration between the nodes. From standard analogy between mechanical and acoustic networks in which force (respectively, velocity) corresponds to acoustic velocity (respectively, acoustic pressure), we further explain how a similar relationship exists here between the panel displacement and the pressure difference at the two nodes. Following a classical modal expansion approach and including the first panel mode only, panel's out-of-plane displacement can be expressed as $W(y,z) = a_{(1,1)}\varphi_{(1,1)}(y,z)$, where $a_{(1,1)}$ is the modal displacement amplitude and $\varphi_{(1,1)}$ is the mode shape function $\varphi_{(1,1)}(y,z) = \sin(\pi y / w)\sin(\pi z / h)$. Since 80Hz is below the first natural frequency, the dynamic behavior of the panel could be characterized by the first mode.

Substituting *W* into the governing equation of panel motion, the displacement amplitude can be obtained as[31]

$$a_{(1,1)} = \frac{\int[(P_1 - P_2)\varphi_{(1,1)}]\mathrm{d}y\,\mathrm{d}z}{m(\omega_{(1,1)}^2 - \omega^2)} = \frac{4wh}{m\pi^2}\frac{(P_1 - P_2)}{(\omega_{(1,1)}^2 - \omega^2)} \tag{1}$$

where P_1 and P_2 are the pressures before and after the panel [probe 1 and probe 2 in Fig. 3 (c)&(d)], m is the modal mass $m = \rho_s t w h / 4$. After rearranging the above equation, the averaged panel displacement can be obtained as

$$\bar{W} = \frac{\int W \, dy \, dz}{w h} = \frac{64}{\rho_s t \pi^4} \frac{(P_1 - P_2)}{(\omega_{(1,1)}^2 - \omega^2)} \tag{2}$$

Since P_1 and P_2 are directly linked to the pressure fields at the two nodes connecting to the main duct, the proposed metamaterial works similar to an inerter, where the inertance is determined by the relative motion of two nodes. The node locations where the panel embedded HQ tube is connected to the inlet and outlet should play an important role in determining the rising peak frequency, as we expect from the wave propagation pattern in the constructed duct network.

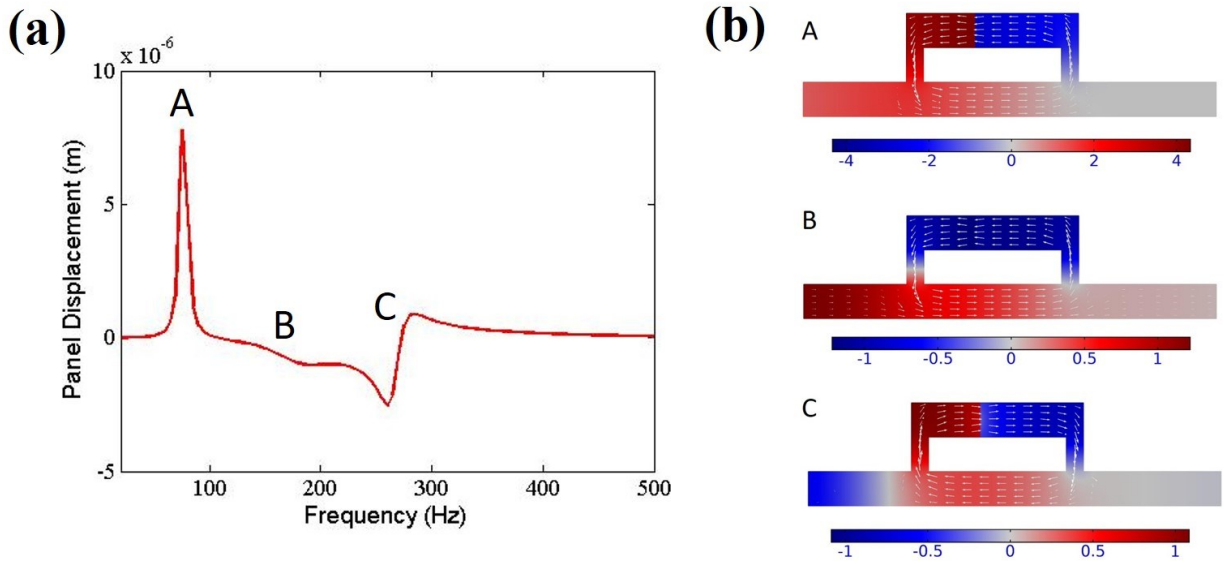

FIG. 4. (a) Simulated vibration displacement of the flexible panel. (b) Simulated sound pressure contours of the acoustic inerter drawn on the *x*-*z* plane, at the three STL peaks, overlaid by sound intensity flow diagrams (directed to the arrows point and valued by their lengths). All simulations are performed by COMSOL Multiphysics.

The surface-averaged panel displacement is shown in Fig. 4(a). As expected, the curve exhibits substantial changes at 80 and 270 Hz, confirming the panel's role at the two peaks. The panel displacement reaches its maxima at 80 Hz, where the sound pressure contour plotted in Fig. 4(b) shows that large sound pressures with opposite signs are driving panel motion. The panel behaves like a piston as its vibration is uniformly distributed over whole surface. Such a piston-like panel is the image of that small mass in a mechanical inerter (see Fig. 1). The energy flow in the acoustic inerter also replicates what can be seen in its mechanical counterpart, as shown in Fig. 4(b). The piston-like motion of the panel pumps the incident acoustic energy in a circulation around the main duct-side branch loop, stopping any sound from travelling downstream. This circulation, if using the terms of a HQ-tube, creates an "infinite" phase lag of the sound pressure, thus pushing the STL peak to an ultra-low frequency. For the second peak at 170 Hz, the pressure difference vanishes and the panel vibrates gently. Note that the first panel mode at 180 Hz overlaps with the original peak of the HQ tube, thus the attenuation peak occurs at the same frequency and inherits the same behavior of destructive interference from the HQ tube. The peak at 270 Hz is most likely due to the structural-acoustic coupling effect, air in one sub-cavity is compressed while in the other it inflates, creating a phase change of sound pressure. This phase change is superimposed on the one already created by the HQ tube, forming the STL peak at 270 Hz.

IV. Conclusion

In summary, we have proposed a new class of acoustic metamaterial by inserting a flexible panel into the side-branch of a Herschel-Quincke tube. We call this new acoustic metamaterial *acoustic inerter* since it is inspired by the mechanical inerter, a widely used device for vibration isolation. With a special focus on a new, ultra-low frequency peak in its sound transmission loss,

the sound attenuation characteristic of the acoustic inerter has been studied by both numerical simulations and experimental investigations. It is found that in contrast to a standard Helmholtz resonator which drains a portion of acoustic energy out of the main duct, the motion of that flexible panel, driven by the drastic sound pressure difference across it, forces the acoustic energy circulate in the loop formed by the acoustic inerter. Being trapped in such a circulation, the incident sound energy couldn't reach the outlet, giving rise to that new peak of sound transmission loss. As a final remark, we point out more efforts are needed to expand the effective bandwidth of the ultra-low frequency peak, which would be the focus of our future work. Potential measures include fine-tuning of design parameters, introducing periodicity into the system, etc.

Acknowledgements

MYZ and YX would like to acknowledge the support from the Career Development Award, Singapore Agency for Science, Technology and Research (grant No. A1820g0092). MYZ also wishes to acknowledge the support from the National Natural Science Foundation of China (No. 51975352).

References

[1] D. Zhao, AIAA journal. **50**, 6 (2012).

[2] X. Yang, J. Yin, G. Yu, L. Peng, and N. Wang, Applied Physics Letters. **107**, 193505 (2015).

[3] M. P. Peiró-Torres, S. Castiñeira-Ibáñez, J. Redondo, and J. V. Sánchez-Pérez, Applied Physics Letters. **114**, 171901 (2019).

[4] X. Yu, Z. Lu, L. Cheng, and F. Cui, Journal of Sound and Vibration. **401**, (2017).

[5] T. Yamamoto, Journal of Applied Physics. **123**, 215110 (2018).

[6] D. P. Jena, J. Dandsena, and V. G. Jayakumari, Applied Acoustics. **155**, (2019).

[7] J. H. Lu, C. C. Kuo, F. L. Hsiao, and C. C. Chen, Applied Physics Letters. **101**, 051907 (2012).

[8] G. S. Liu, Y. Y. Peng, M. H. Liu, X. Y. Zou, and J. C. Cheng, Applied Physics Letters. **113**, 153503 (2018).

[9] A. Isozaki, H. Takahashi, H. Tamura, T. Takahata, K. Matsumoto, and I. Shimoyama, Applied Physics Letters. **105**, 241907 (2014).

[10] Y. Li and B. M. Assouar, Applied Physics Letters. **108**, 063502 (2016).

[11] R. Ghaffarivardavagh, J. Nikolajczyk, S. Anderson, and X. Zhang, Physical Review B. **99**, 024302 (2019).

[12] X. Yu, Z. Lu, T. Liu, L. Cheng, J. Zhu, and F. Cui, Journal of Sound and Vibration. **449**, 2019.

[13] C. J. Naify, C. M. Chang, G. McKnight, F. Scheulen, and S. Nutt, Journal of Applied Physics. **109**, 104902 (2011).

[14] X. Wang, H. Zhao, X. Luo, and Z. Huang, Applied Physics Letters. **108**, 041905 (2016).

[15] Y. Liu, and J. Du, Journal of Applied Physics. **125**, 034901 (2019).

[16] W. W. Yu, L. Fan, R. H. Ma, H. Zhang, and S. Y. Zhang, Applied Physics Letters. **112**, 183506 (2018).

[17] X. Wang, X. Luo, H. Zhao, and Z. Huang, Applied Physics Letters. **112**, 021901 (2018).

[18] Y. Wu, M. Yang, and P. Sheng, Journal of Applied Physics. **123**, 090901 (2018).

[19] M. C. Smith, IEEE Transactions on Automatic Control. **47**, (2002).

[20] P. Brzeski, T. Kapitaniak, and P. Perlikowski, Journal of Sound and Vibration. **349**, (2015).

[21] Y. Shen, L. Chen, X. Yang, D. Shi, and J. Yang, Journal of Sound and Vibration. **361**, (2016).

[22] C. Yilmaz, G. M. Hulbert, and N. Kikuchi, Physical Review B. **76,** 054309 (2007).

[23] C. Yilmaz and G. M. Hulbert, Physics Letters A. **374**, (2010).

[24] S. Taniker and C. Yilmaz, International Journal of Solids and Structures. **72**, (2015).

[25] O. Yuksel and C. Yilmaz, Journal of Sound and Vibration. **355**, (2015).

[26] N. M. Frandsen, O. R. Bilal, J. S. Jensen, and M. I. Hussein, Journal of Applied Physics. **119**, 124902 (2016).

[27] J. Li and S. Li, Physics Letters A. **382**, (2018).

[28] J. Li, P. Yang and S. L, Composite Structures. **231**, (2020).

[29] J. Zhou, L. Dou, K. Wang, D. Xu, and H. Ouyang, Nonlinear Dynamics. **96**, (2019).

[30] A. Selamet, N. S. Dickey, and J. M. Novak, The Journal of the Acoustical Society of America. **96**, (1994).

[31] X. Yu, L, Cheng, J. L. Guyader, The Journal of the Acoustical Society of America, **136**, (2014)